Journal of Sound and Vibration (1997) **201**(3), 365–381

SYMMETRY IN THE PROBLEM OF VIBRATION OF A POLAR-ORTHOTROPIC NON-HOMOGENEOUS PLATE ON AN ELASTIC FOUNDATION

B. KLYACHKO AND S. KLYACHKO

Victorian Writers' Centre Inc., 156 *George Street*, *Fitzroy*, *Victoria* 3065, *Australia*

(*Received* 13 *June* 1994, *and in final form* 9 *September* 1996)

The problem of bending vibration of a polar-orthotropic non-homogeneous elastic plate on an elastic foundation is considered, and the invariance of the problem-equation under an inversion transformation with respect to a circle is proved. As a corollary, the optimization problem (the "best" position of the point mass or point support, which optimizes the plate fundamental frequency) is considered and certain geometrical inequalities, which reduce the optimization domain, are proved. Computational time economy generated by the inequalities for the optimization problem is illustrated with numerical examples: (a) the "best" position of the point mass on segment and ring-sector plates; (b) the "best" radius of the ring support for annular plates. Some other corollaries from the problem-equation inversion invariance are given.

1. INTRODUCTION

The problem of the bending dynamics of a polar-orthotropic non-homogeneous elastic plate on an elastic foundation is considered. This problem is relevant to the design of various structural members. It is proved that the problem-equation is invariant under an inversion transformation with respect to a circle. On this basis, certain corollaries which may be used in design are proved. The corollaries are illustrated with numerical examples.

The paper consists of two parts. Sections 2–7 of the main part are as follows: 2. Invariance of the problem-equation; 3. Optimal mass position; 4. Numerical examples of optimal mass position; 5. Optimal support position; 6. Numerical examples of optimal support position; 7. Generalizations. The auxiliary part consists of Appendices 1–6 to sections 2–7, respectively, which contain proofs, some corollaries and additional materials.

In section 2, the mathematical description of the bending dynamics problem is given and the application of the geometrical inversion transformation is considered. The use of inversion for problems of plate bending and 2-D elasticity has been considered in many works [1–9]. Here it is assumed that orthotropy tensor components are constant along the radius and are arbitrary functions of the angular co-ordinate. One then has the result that if two tensor components satisfy only one condition (namely that the sum of these two components is constant), then the problem-equation is invariant under inversion. Examples of industrially used materials which practically satisfy this only one condition of invariance are given.

0022–460X/97/130365 + 17 $25.00/0/sv960767

In section 3, the optimization problem of the "best" position of a point mass on the plate, which minimizes the plate eigenfrequency, is considered and, as a corollary from section 2, the geometrical inequality is given. It is proved that if the plate is inversion symmetric with respect to the circle (the "number" of such plates is infinite—like the "number" of plates which are mirror symmetric with respect to a straight line), then a search for the "best" mass position may be made only in part of plate domain.

In section 4, the computational time economy generated by the inequality of section 3 in the optimization process is illustrated by numerical examples: the "best" point mass position on segment and ring-sector plates. Numerical values of the time economy are given.

In section 5, the optimization problem of the "best" position of a point support, which maximizes the plate fundamental frequency, is considered and (also as for the corollary from section 2) the inequality which reduces the domain of optimization is proved.

In section 6, the computational time economy generated by the inequality of section 5 in the optimization process is illustrated by a numerical example: the "best" radius of a ring support for annular plates in case of axisymmetric vibration.

Section 6 is, in some sense, a "paper within a paper"—it contains the detailed numerical contribution to the annular plate vibration problem, which is the theme of many publications. The plate fundamental frequency is calculated as a function of the support radius in the whole interval between the inner and outer radii of the annular plate, for the respective plate parameters (characteristics of the orthotropy tensor, elastic support and mass distribution). The numerical method used is tested by comparison with exact results and with results given in other publications. Therefore, the section 6 results may be considered as useful for design (independently of the main theme of the paper).

From the point of view of the theme, the main corollary from this "paper within a paper", i.e., section 6, is the illustration of the "theoretical" result of section 5: all "best" radii calculated in section 5 satisfy the inequality proved in section 5. Therefore, for their determination it is sufficient to scan only part of the interval between the inner and outer radii of the plate. Numerical values of the time economy are given.

In section 7, generalizations and some other corollaries from the problem-equation invariance are noted (applications to non-inversion-symmetric plates, impact problem, forced vibration, viscoelastic materials, etc.).

2. INVARIANCE OF THE PROBLEM-EQUATION

(i) Dynamic bending of a polar-orthotropic non-homogeneous elastic plate on an elastic foundation is considered. Plate domain A is bounded, simply- or multiply connected, and of arbitrary shape. Let r, θ be polar co-ordinates with origin $O \notin A + \partial A$. It is given as follows: on ∂A—kinematic conditions (w, $\partial w/\partial n$ as a functions of position and t); and in A $(w)_{t=0}$, $(\partial w/\partial t)_{t=0}$ and load $q(r, \theta, t)$. (Here and below the commonly used symbols are not explicitly defined.) The plate rigidity tensor is such that its "physical" co-ordinates (i.e., co-ordinates in the local orthonormal basis of the r, θ system) are functions only of θ: $D^{ijkl} = D^{ijkl}(\theta)$, where $D^{1111} = D_{11}$, $D^{2222} = D_{22}$, $D^{1122} = D_{12}$ and $D^{1212} = D_{66}$. In the isotropy case $D^{1111} = D^{2222} = D = Eh^3/(12(1-\mu^2))$, $D^{1122} = \mu D$ and $D^{1212} = (1/2)(1-\mu)D = Gh^3/(12(1-\mu^2))$. The problem-equation (see, e.g., reference [10]) is rewritten as follows in a form that is convenient for the invariance proof:

$$D^{1111}w_{,rrrr} + 2D_0 r^{-2}w_{,rr\theta\theta} + D^{2222}r^{-4}w_{,\theta\theta\theta\theta}$$

$$+ 2D^{1111}r^{-1}w_{,rrr} + 2D_{0,\theta}r^{-2}w_{,rr\theta} - 2D_0 r^{-3}w_{,r\theta\theta}$$

$$+ 2D^{2222}_{,\theta} r^{-4} w_{,\theta\theta\theta} + (D^{1122}_{,\theta\theta} - D^{2222}) r^{-2} w_{,rr}$$

$$+ 2(D^{2222} - 2D^{1212})_{,\theta} r^{-3} w_{,r\theta} + (D^{2222}_{,\theta\theta} + 2D^{2222} + 2D_0) r^{-4} w_{,\theta\theta}$$

$$+ (D^{2222}_{,\theta\theta} + D^{2222}) r^{-3} w_{,r} + 4D^{1212}_{,\theta} r^{-4} w_{,\theta} = q - cw - m w_{,tt}. \tag{2.1}$$

Here $D_0 = D^{1122} + 2D^{1212}$, $(\ *)_{,r} \equiv \partial(\ *)/\partial r$, $(\ *)_{,\theta} \equiv \partial(\ *)/\partial\theta$, and so on.

(ii) Let there be a circle with radius ρ $(0 < \rho < \infty)$ and centre at O. One can write the following transformation based on geometrical inversion-mapping [2, 4]:

$$r = \rho^2/r^*, \qquad \theta = \theta^*, \qquad \mathrm{d}S = p^4\,\mathrm{d}S^*, \qquad p = \rho/r^*, \qquad t = t^*,$$

$$w(r, \theta, t) = p^2 w^*(r^*, \theta^*, t^*), \qquad q(r, \theta, t) = p^{-6} q^*(r^*, \theta^*, t^*),$$

$$c(r, \theta) = p^{-8} c^*(r^*, \theta^*), \qquad m(r, \theta) = p^{-8} m^*(r^*, \theta^*). \tag{2.2}$$

Here and below a symbol with an asterisk denotes a result of transformation.

It is possible to show (see Appendix 1) that if D^{1111}, D^{2222} and D^{1212} are arbitrary functions of θ and $D^{1122} = C - D^{2222}$, where C is an arbitrary constant, then equation (2.1) is invariant under transformation (2.2).

On this basis, all inversion applications used in various problems for isotropic homogeneous plates [1–9] may be used for plates of type (2.1). In other words, there is a one-to-one correspondence between problems for polar-orthotropic non-homogeneous plate A and its inversion image A^* (see Figure 1).

(iii) The material condition

$$D^{1122}(\theta) + D^{2222}(\theta) = \text{constant}. \tag{2.3}$$

(iii, 1) Each plate with any arbitrary $D^{ijkl} = \text{constant}$ satisfies equation (2.3). Each plate with $D^{ijkl}(\theta) \neq \text{constant}$, which satisfies equation (2.3) and (otherwise) is arbitrary, may be fabricated by use of reinforcement, composites, structural orthotropy, etc.

(iii, 2) Consider a reinforcement plate. It is known that if (a) the reinforcement "acts" in only the r-direction, (b) the reinforcement coefficient is varied in only the θ-direction, and (c) the "main" (before reinforcement) material is homogeneous, then $D^{1111}(\theta)$ varies with θ significantly and other D^{ijkl} vary weakly. Therefore, in that very well known case, it is possible to accept $D^{1122}(\theta) + D^{2222}(\theta) \approx \text{constant}$ and exploit the benefits generated by the inversion-invariance of equation (2.1). Numerical examples of such materials are given in Appendix 1.

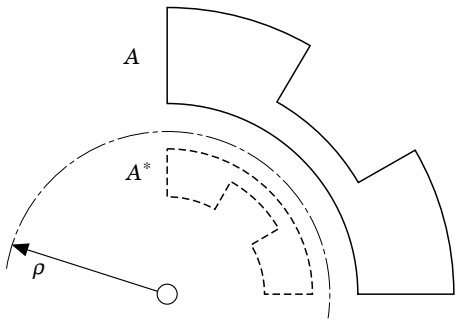

Figure 1. A polar-orthotropic non-homogeneous plate A and its inversion image A^*.

3. OPTIMAL MASS POSITION

Consider now a polar-orthotropic non-homogeneous plate that is inversion-symmetric with respect to the circle with radius r_s ($0 < r_s < \infty$): that is, $A^* = A$ and $\partial A^* = \partial A$. Such domains form an infinite class (as do domains which are mirror-symmetric with respect to a straight line). Many "classical" domains belong to this class: circles, co- and eccentric rings, ring sectors, segments, all lunes, and so on. Members with such domains are used in various structures. We remark that the radius of the circle of inversion is denoted as r_s only if this circle is a circle of symmetry (i.e., if $\partial A^* = \partial A$); in the general case the notation ρ is used—see section 2.

The plate contour is rigidly clamped. For brevity, an elastic foundation and distributed mass are absent. The concentrated mass M is fastened to the plate at the point $\alpha_M(r_M, \theta_M)$; the plate material density is neglected, so

$$m(r, \theta) = M\delta(r - r_M, \theta - \theta_M), \tag{3.1}$$

and one has a system "inertialess plate–point mass". The eigenfrequency of the system depends on the position of α_M: $\omega = \omega(\alpha_M)$.

Consider the following optimization problem: find point (points) $\alpha_{Mmin}(r_{Mmin}, \theta_{Mmin})$ such that for all points α_M one has $\omega(\alpha_M) \geqslant \omega(\alpha_{Mmin})$.

It is possible to show (see Appendix 2) that

$$r_{Mmin} > r_s. \tag{3.2}$$

Inequalities for a group of similar optimization problems are also given in Appendix 2. Inequality (3.2) narrows the area of searching, i.e., it reduces the search time, and therefore may be used in optimization.

4. NUMERICAL EXAMPLES OF OPTIMAL MASS POSITION

Although expression (3.2) is valid for any irregular $\partial A = \partial A^*$, it is clear that for illustration it is sufficient to consider plates of only "classical" shape.

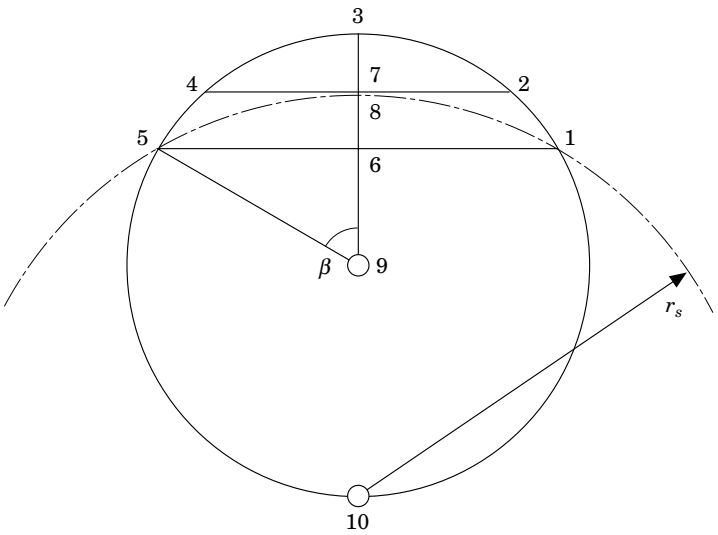

Figure 2. The segment plate geometry.

(i) Consider a plate, the domain of which is the segment 1–2–3–4–5–6 with $0 < \beta < \pi$ (see Figure 2). At first, assume that the plate is isotropic and homogeneous.

Let $d[i, j]$ denote the relative distance between points i, j such that $d[3, 6] = 1$, $d[7, 6] = 0{\cdot}5$ and $x = d[\alpha_{Mmin}, 6]$ is a search distance (relative) from the "weakest" point of the plate to point 6. From the physics point of view α_{Mmin} is on line 3–7–6 between points 7 and 6 (because the part 2–7–4–5–6–1 of plate is "weaker" than part 2–3–4–7), so $0 < x < 0{\cdot}5$.

However, the segment has a circle of inversion-symmetry with a centre at 10, so (according to inequality (3.2)) the point α_{Mmin} is between points 7 and 8, and so $d[8, 6] < x < 0{\cdot}5$.

Consider two segments (two plates). After calculations one has: $\beta = 90^\circ$ (semi-circle) $d[8, 6] = 0{\cdot}414 < x < 0{\cdot}5$; $\beta = 60^\circ$ (see the scale in Figure 2) $d[8, 6] = 0{\cdot}464 < x < 0{\cdot}5$.

One sees that inequality (3.2) decreases significantly the volume of searching. Note that we do not refer here to the many publications with solutions of this problem. We only use this problem as an evident illustration. Inequality (3.2) is also true for any polar-orthotropic non-homogeneous plate with condition (2.3).

(ii) Let the optimization time economy generated by expression (3.2) be $\aleph = F'/F$, where F is the full area of optimization (without considering expression (3.2)) and F' is the "useless" area (according to expression (3.2)). Therefore, the values 1, $\aleph$ and $1 - \aleph$ relate to the full time, saved time and the "true" time (i.e., the time of searching the "useful" subdomain), respectively. Such an expression for $\aleph$, based on proportionality between time and area, is a rough approximation, but for purposes here it is sufficient. For segment-plates with $\beta = 90^\circ$ and 60° one has $\aleph_{90} = 0{\cdot}414/0{\cdot}5 = 82{\cdot}8\%$ and $\aleph_{60} = 0{\cdot}464/0{\cdot}5 = 92{\cdot}8\%$. It is more correct for the evaluation of inequality (3.2) to omit the additional information $x < 0{\cdot}5$ and assume $F = 1$; then one obtains smaller, but more adequate values of time economy: $\aleph_{90} = 0{\cdot}414/1 = 41{\cdot}4\%$ and $\aleph_{60} = 0{\cdot}464/1 = 46{\cdot}4\%$.

(iii) Consider a polar-orthotropic homogeneous plate, the domain A of which is a sector of a concentric ring with radii $\infty > R_{out} > R_{int} > 0$ and central angle $2\beta > 0$. A corollary from inequality (3.2) is as follows: for any values of D_{ij}, R_{out}, R_{int} and β, $r_{Mmin} > r_s = (R_{out} R_{int})^{1/2}$. This is also valid for any $D^{ijkl}(\theta)$ with condition (2.3). In the case considered the economy in optimization time is $\aleph = F'/F = (r_s - R_{int})/(R_{out} - R_{int})$. If, for example, $R_{int}/R_{out} = 0{\cdot}5$, then $\aleph = 41{\cdot}4\%$; if $R_{int}/R_{out} = 0{\cdot}2$, then $\aleph = 30{\cdot}9\%$.

Note that $\aleph \leqslant 50\%$. The limit value $\aleph = 50\%$ corresponds to $r_s = \infty$: i.e., to the case of a domain which is mirror-symmetric with respect to a straight line. Inequality (3.2) is valid not only for inversion-symmetric plates (see Appendix 3).

5. OPTIMAL SUPPORT POSITION

Consider a plate with inversion-symmetric domain A and with inversion-symmetric mass distribution (ISMD). A distributed elastic foundation is absent (for brevity). What is the ISMD? One can consider it in detail. There is a close analogy between ISMD and a mirror-symmetric mass distribution for a plate, which is geometrically mirror-symmetric with respect to a straight line. In our case of inversion symmetry the function for, say, $r \leqslant r_s$ $m_{int}(r, \theta)$ may be given arbitrarily; then the function for $r \geqslant r_s$ $m_{out}(r, \theta)$ is obtained as the inversion image of $m_{int}(r, \theta)$ (see expression (2.2)): $m_{out}(r, \theta) = (r_s/r)^{+8} m_{int}(r_s^2/r, \theta)$. Therefore, any function $m(r, \theta) = \{r \leqslant r_s: m_{int}(r, \theta); r \geqslant r_s: m_{out}(r, \theta)\}$ is an ISMD. In other words, the set of them is the infinite set of solutions of the functional equation $m(r, \theta) = (r_s/r)^8 m(r_s^2/r, \theta)$. (Compare this with the mirror-symmetric mass distribution, which is the solution of the functional equation $m(x, y) = m(x, -y)$, where x and y are orthonormal co-ordinates.)

As an example of ISMD, let $m_{int}(r, \theta) = f(\theta)$, where $f(\theta)$ is arbitrary; then $m_{out}(r, \theta) = (r_s/r)^8 f(\theta)$, and then $m(r, \theta) = \{r \leqslant r_s : f(\theta);\ r \geqslant r_s : (r_s/r)^8 f(\theta)\}$ is the ISMD.

So, one has a plate with ISMD. Let that plate have an elastic support with rigidity $C \leqslant \infty$ in point $\alpha_C(r_C, \theta_C)$. It is clear that $\omega^{(i)} = \omega^{(i)}(\alpha_C)$.

Consider the following optimization problem: find the point (at least one) $\alpha_{Cmax}(r_{Cmax}, \theta_{Cmax})$ such that, for all α_C, $\omega^{(1)}(\alpha_C) \leqslant \omega^{(1)}(\alpha_{Cmax})$. (For brevity, the simplified formulation is given here.)

It is possible to prove (see Appendix 4) that there exists point α_{Cmax} with

$$r_{Cmax} \geqslant r_s. \tag{5.1}$$

(We remark that if $C = \infty$, then all "maximal" points are disposed symmetrically with respect to symmetry-circumference.)

Now let the plate have a system of N absolutely rigid supports at points $\alpha_C = \{\alpha_{Ci}\}$. As above, it is clear that $\omega^{(i)} = \omega^{(i)}(\alpha_C)$.

Consider the following optimization problem: find the point-system α_{Cmax} such that, for all other point-systems α_C, $\omega^{(1)}(\alpha_C) \leqslant \omega^{(1)}(\alpha_{Cmax})$.

It is possible to prove that if some point-system is "maximal", then its inversion-image is also the "maximal" point-system. Analogous statements may be formulated in cases of a prearranged internal domain $B \subset A$ and in cases of system of supports with $C_i < \infty$.

6. NUMERICAL EXAMPLES OF OPTIMAL SUPPORT POSITION

The aim of the examples is to illustrate the reduction of the domain of searching. Consider an annular plate (bounded by two concentric circumferences) with clamped edges and with an additional elastic support, which is uniformly distributed along the circumference with radius r_{sup}. The support circumference is concentric with the plate contour. The aim of the problem is to find the optimal value of r_{sup}, which maximizes $\omega^{(1)}$. At first consider the case of an inversion-symmetric mass distribution (ISMD), that is a non-uniform distribution, and thereafter the "illustration" is extended to the case of a uniform mass distribution.

Plates with such additional intermediate "line-wise" elastic supports are often used as members of various structures; see, e.g., reference [11]. Note that reference [11] also deals with optimization, but there the position of a line elastic support (or supports) is (are) given and the best orientation of anisotropy of plate material is determined: such an orientation which maximizes the eigenfrequency $\omega^{(1)}$. Here the plate anisotropy is fixed and the radius r_{sup} of the "circumference–elastic–support", which maximizes $\omega^{(1)}$, must be obtained. One can also note reference [12], where the optimal position of "point-wise" additional supports is investigated, and references [13–18], where the circular, annular, isotropic and orthotropic plates with concentric support ring (rings) and non-inversion-symmetric mass distribution are considered and where the functions $\omega^{(i)}(r_{sup})$ are investigated.The studies in references [13–18] were made for various values of the problem parameters (D^{ijkl}, support stiffness, boundary conditions, plate thickness geometry functions $h(r)$, etc.) and by various calculation methods. Some of those results are used below for testing of numerical method used in this section.

The contents of this section are as follows: (i) Problem description; (ii) Results and discussion; (iii) Conclusion. The numerical method description, with its testing and some corollaries, is given in Appendix 5.

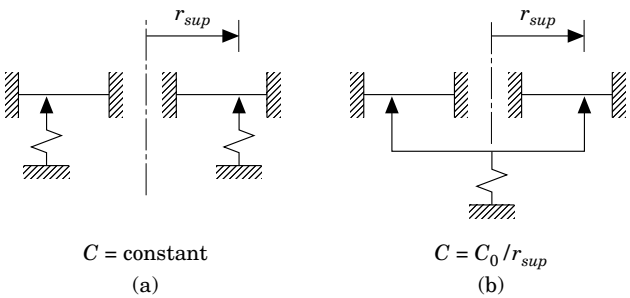

Figure 3. Examples for the optimization problem of "best" r_{sup}: (a) C is independent of r_{sup} and is a given constant; (b) C is inversely proportional to r_{sup} (C_0 is a given constant). C denotes the support stiffness (related to the unit of length of the support circumference).

(i) PROBLEM DESCRIPTION

The plate domain is the ring with $0 < r_{int} \leqslant r \leqslant r_{out} < \infty$. The radius of inversion symmetry $r_s = (r_{int}r_{out})^{1/2}$. Only axisymmetric eigenvibrations $w(r)\sin(\omega^{(1)}t)$ are considered (up to the end of this section, w is the eigenfunction). The boundary conditions are

$$r = r_{int}: \qquad w = 0, \quad w_{,r} = 0; \qquad\qquad r = r_{out}: \qquad w = 0, \quad w_{,r} = 0. \tag{6.1, 6.2}$$

The plate has an inversion-symmetric mass distribution (ISMD). To construct the ISMD one can (see the previous section) arbitrarily assume $m_{out}(r)$ for, e.g., the subdomain $r_s \leqslant r \leqslant r_{out}$. Let, e.g., $m_{out} = \text{constant} = m_0$. Then, for subdomain $r_{int} \leqslant r \leqslant r_s$, one obtains the m_{int} as an inversion image of m_{out}: i.e. (from expression (2.2)), $m_{int} = (r_s/r)^{+8}m_0$, and

$$m(r) = m_{int}(r) \cup m_{out}(r) = \{r \leqslant r_s: (r_s/r)^{+8}m_0;\ r \geqslant r_s: m_0\}. \tag{6.3}$$

The problem-equation is (from equation (2.1))

$$D^{1111}w_{,rrrr} + 2D^{1111}r^{-1}w_{,rrr} - D^{2222}r^{-2}w_{,rr} + D^{2222}r^{-3}w_{,r} = -c(r)w + \omega^2 mw, \tag{6.4}$$

where D^{ijkl} relates to the local orthonormal basis, m relates to the area unit, $c(r) = C\delta(r - r_{sup})$ and where C is the elastic support stiffness related to the unit of length. The results of section 5 are valid for the case (a) $\partial C/\partial r_{sup} = 0$ and for the class of functions $C(r_{sup})$, particularly for the case (b) $\partial[2\pi r_{sup}C(r_{sup})]/\partial r_{sup} = 0$; that is, $C(r_{sup}) = C_0/r_{sup}$. Both cases (a) and (b) have simple mechanical reference (see Figures 3(a) and (b)); below, for brevity, only case (a) will be considered.

TABLE 1

$\lambda = \omega^{(1)}(m_0/D^{1111})^{1/2}(r_{out})^2$ *versus* C_{nd} *for case* $m_{nd} \equiv 1$, $D_{nd}^{2222} = 1$, $\xi_{sup} = 0{\cdot}75$

C_{nd}	λ
0	89·25
10^{+1}	89·53
10^{+2}	92·03
10^{+3}	113·58
10^{+4}	219·31
10^{+5}	246·34
∞	246·34

Consider the following optimization problem (a particular case of the problem of section 5): find $r_{sup\,max}$ (at least one value) such that, for all r_{sup}, the inequality $\omega^{(1)}(r_{sup}) \leqslant \omega^{(1)}(r_{sup\,max})$ is valid.

According to the corollary from section 5, there exists $r_{sup\,max} \geqslant r_s$. To illustrate this corollary, the functions $\omega^{(1)} = \omega^{(1)}(r_{sup})$ for various plate parameters will be calculated.

One can introduce the non-dimensional quantities

$$\xi = r/r_{out}, \qquad \xi_{int} = \ldots, \qquad \xi_{sup} = \ldots, \qquad \xi_{out} = 1, \qquad \xi_s = r_s/r_{out} = (\xi_{int})^{1/2},$$

$$D_{nd}^{2222} = D^{2222}/D^{1111},$$

$$\lambda = \omega^{(1)}(m_0/D^{1111})^{1/2}(r_{out})^2, \qquad m_{nd}(\xi) = m(r_{out}\xi)/m_0, \qquad w_{nd}(\xi) = w(r_{out}\xi),$$

$$\delta(\xi - \xi_{sup}) = r_{out}\,\delta(r_{out}\xi - r_{out}\xi_{sup}), \qquad C_{nd} = (C/D^{1111})(r_{out})^3, \tag{6.5}$$

and rewrite expressions (6.4), (6.1) and (6.2). For calculation the plate domain is divided into two parts, A ($\xi \leqslant \xi_{sup}$) and B ($\xi \geqslant \xi_{sup}$) and the member $-C_{nd}\delta(\xi - \xi_{sup})w_{nd}$ (which appears in the equation after non-dimensionalization) is relocated from the equation into the junction condition. Therefore one has two functions w_{nd}^A and w_{nd}^B, which are defined on the subdomains A and B respectively and which satisfy

$$w_{nd,\xi\xi\xi\xi} + 2\xi^{-1}w_{nd,\xi\xi\xi} - D_{nd}^{2222}\xi^{-2}w_{nd,\xi} + D_{nd}^{2222}\xi^{-3}w_{nd,\xi} = \lambda^2 m_{nd}(\xi)w_{nd}, \tag{6.6}$$

$$\xi = \xi_{int}: \qquad w_{nd}^A = 0, \quad w_{nd,\xi}^A = 0; \qquad \xi = 1: \qquad w_{nd}^B = 0, \quad w_{nd,\xi}^B = 0; \tag{6.7, 6.8}$$

$$\xi = \xi_{sup}: \qquad w_{nd}^A = w_{nd}^B, \quad w_{nd,\xi}^A = w_{nd,\xi}^B, \quad w_{nd,\xi\xi}^A = w_{nd,\xi\xi}^B, \tag{6.9}$$

$$w_{nd,\xi\xi\xi}^B = w_{nd,\xi\xi\xi}^A - C_{nd}w_{nd}^A. \tag{6.10}$$

The problem is solved by the initial-parameters method, and using the Runge–Kutta algorithm. The method is tested by comparison with "exact" method results based on using Bessel function approximations [19–21]; the results are shown in Table 1. Because the modulus of the differences between the respective eigenfrequency parameters is less than 0·001, the data given in Table 1 belongs to both (numerical and "exact") methods. The present numerical method is denoted as method N and the "exact" one as method E. Method N is also tested by comparison with results of references [17, 18, 22–24]. A detailed description of method N with its testing is given in Appendix 5.

TABLE 2

$\lambda = \omega^{(1)}(m_0/D^{1111})^{1/2}(r_{out})^2$ *versus* ξ_{sup} *for case* $m = m(r)$

	$D_{nd}^{2222} = 1$		$D_{nd}^{2222} = 10$		$D_{nd}^{2222} = 0{\cdot}1$	
ξ_{sup}	$C_{nd} = 5000$	$C_{nd} = \infty$	$C_{nd} = 5000$	$C_{nd} = \infty$	$C_{nd} = 5000$	$C_{nd} = \infty$
0·50	78·45	78·45	82·49	82·49	78·03	78·03
0·55	80·71	99·14	84·70	103·28	80·30	98·71
0·60	95·11	124·72	98·71	128·94	94·74	124·29
0·65	118·96	156·54	121·92	160·87	118·66	156·10
0·70	143·07	187·63	145·12	192·36	142·86	187·15
0·75	137·93	168·43	140·71	172·86	137·65	167·98
0·80	118·84	139·76	122·27	144·03	118·49	139·33
0·85	101·71	118·20	105·43	122·40	101·33	117·77
0·90	87·92	101·73	91·82	105·88	87·51	101·30
0·95	79·69	88·78	83·71	92·87	79·27	88·36
1·00	78·45	78·45	82·49	82·49	78·03	78·03

TABLE 3

Optimal radii $\xi_{sup\,max}$ and maximal eigenfrequencies λ_{max}

D_{nd}^{2222}	C_{nd}	$\xi_{sup\,max}$	λ_{max}
1	∞	$\xi_s = (2)^{-1/2}$	188·54
1	5000	0·716	145·65
10	∞	$\xi_s = (2)^{-1/2}$	193·29
10	5000	0·717	147·70
0·1	∞	$\xi_s = (2)^{-1/2}$	188·05
0·1	5000	0·716	145·44

(ii) RESULTS AND DISCUSSION

Consider an annular plate, the domain of which is a concentric ring with radii $\xi_{int} = 0{\cdot}5$ and $\xi_{out} = 1$. The radius of geometrical symmetry $\xi_s = (\xi_{int}\xi_{out})^{1/2} = (0{\cdot}5)^{1/2}$. The plate has ISMD (6.3). Values of λ for $D_{nd}^{2222} = \{1; 10; 0{\cdot}1\}$, $C_{nd} = \{\infty; 5{\cdot}0e + 3; 0\}$ and support positions $\xi_{sup} = \{0{\cdot}5; 0{\cdot}55; \ldots; 0{\cdot}95; 1\}$ obtained by the N-method are given in Table 2. Optimal support positions $\xi_{sup\,max}$ (such that $d\lambda/d\xi_{sup} = 0$) and corresponding maximal eigenfrequencies λ_{max} obtained also by the N-method are given in Table 3 (note that prepared Turbo–Pascal-realization of the N-method is applicable to all of the parametric space).

For comparison λ for the plate has been calculated, with the same set of initial data, but with uniform mass distribution $m_{nd} = 1$ (a discussion of this is given in Appendix 5). The results obtained by the N-method (case $D_{nd}^{2222} = 1$ is obtained by both methods N and E) are shown in Table 4. For this plate the values of $\xi_{sup\,max}$ are very near to 0·75 and values of λ_{max} are very near to $\lambda(0{\cdot}75)$, as shown in Table 4.

The results of Tables 2–4 (i.e., $\lambda(\xi_{sup})$ polygon-like approximations) are partly illustrated in Figure 4 (the accuracy level of Figure 4 is less than that of the tables). As is clear from Tables 2 and 3 and Figure 4 in all cases of inversion-symmetric plates $\xi_{sup\,max} \geqslant \xi_s$. Therefore, one could search for the optimal point not over the whole domain $\{0{\cdot}5, 1\}$, but only over the subdomain $\{0{\cdot}707, 1\}$. This is an illustration of the results of section 5. The economy in time (i.e., "saved" time) is $\aleph = (0{\cdot}707 - 0{\cdot}5)/0{\cdot}5 = 41{\cdot}4\%$.

TABLE 4

$\lambda = \omega^{(1)}(m_0/D^{1111})^{1/2}(r_{out})^2$ versus ξ_{sup} for case $m =$ constant

	$D_{nd}^{2222} = 1$		$D_{nd}^{2222} = 10$		$D_{nd}^{2222} = 0{\cdot}1$	
ξ_{sup}	$C_{nd} = 5000$	$C_{nd} = \infty$	$C_{nd} = 5000$	$C_{nd} = \infty$	$C_{nd} = 5000$	$C_{nd} = \infty$
0·50	89·25	89·25	93·82	93·82	88·78	88·78
0·55	91·03	105·01	95·52	109·37	90·57	104·56
0·60	103·18	127·00	107·19	131·28	102·77	126·56
0·65	125·12	158·60	128·51	163·92	124·78	158·16
0·70	153·79	204·20	156·45	208·83	153·52	203·73
0·75	174·66	246·34	176·95	252·65	174·43	245·70
0·80	153·73	204·10	157·57	210·52	153·33	203·45
0·85	125·07	158·52	129·43	164·25	124·62	157·94
0·90	103·16	126·95	107·67	132·16	102·69	126·42
0·95	91·03	104·99	95·59	109·81	90·56	104·49
1·00	89·25	89·25	93·82	93·82	88·78	88·78

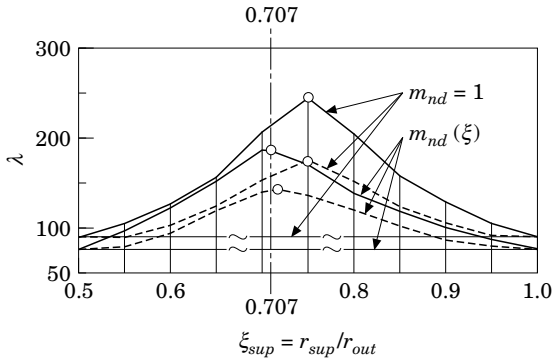

Figure 4. (extracted from Tables 2–4). The eigenfrequency parameter λ versus support position ξ_{sup} for isotropic plate ($D_{nd}^{2222} = 1$) for cases of uniform and non-uniform mass distribution ($m_{nd} = 1$ and $m_{nd} = m_{nd}(\xi)$). C_{nd} values: $- \sim -$, 0; $- - - -$, 5000; ——, ∞. ○, λ_{max}.

As the "side" effect generated by these examples (Tables 1–4), note that the orthotropy change in the range $0{\cdot}1 \leqslant D_{nd}^{2222} \leqslant 10$ and the support rigidity change in the ranges $\{0 \leqslant C_{nd} \leqslant 10^{+1}\}$, $\{10^{+5} \leqslant C_{nd} \leqslant \infty\}$ have little influence on the fundamental eigenfrquency of axisymmetric vibrations of the plates considered here.

(iii) CONCLUSION

Here some of the results of this section are restated.

(iii, 1) For axisymmetric vibration of a clamped–clamped annular orthotropic plate, the functions $\lambda(\xi_{sup})$ have been given. As was noted at the beginning of this section, the vibration problems for annular plates considered are of engineering interest and have been considered in a number of publications (e.g., the analogous relations between eigenfrequency parameters $\lambda^{(1)} \equiv \lambda$, $\lambda^{(2)}$, $\lambda^{(3)}$ and ξ_{sup} for axisymmetric vibration of an annular isotropic plate simply supported at both edges with $\xi_{int} = 0{\cdot}1$ and $m_{nd} = 1$ are given in reference [18]). Thus, the data given in Tables 1–4 and Figure 4 may be useful.

(iii, 2) The "main" result of this section (from the point of view of the aim of this paper) is the numerical illustration of inequality (5.1). Examples show that if it is necessary to find only the $\xi_{sup\,max}$ with λ_{max} (but not the whole function $\lambda(\xi_{sup})$), then one need search only the subdomain $\xi_{sup} \geqslant \xi_s$. This provides a significant reduction of calculation time. For the case $\xi_{int} = 0{\cdot}5$ the saved time $\aleph = 41{\cdot}4\%$. Extensions of this result to the case of non-inversion-symmetric plates are noted in Appendix 5.

7. GENERALIZATIONS

Here some additional corollaries from the inversion-invariance of equation (2.1) are briefly noted.

(i) If plate domain A, mass distribution $m(r, \theta)$ and elastic foundation stiffness coefficient $c(r, \theta)$ are inversion-symmetric, then the general problem may be easy split into two, symmetric and antisymmetric (in the sense of relations (2.2)). The proof is analogous to the proof in the case of mirror-symmetry with respect to a straight line. The usefulness of such splitting is well known. This has the following "physical" corollary: each antisymmetric eigenfunction has a zero-line, which coincides with the circumference of inversion symmetry; analogous symmetrization is possible for each dynamical initial boundary value problem.

(ii) Each plate with any geometrical form (in general, without inversion-symmetry) and with

$$m(r) = H/r^8, \qquad c(r) = K/r^8, \tag{7.1}$$

where H and K are arbitrary factors, is isospectral to a plate with constant m and c. With the help of this statement, one can obtain the exact spectrum (values and functions) for non-uniform m and c, through the known spectrum of a plate with uniform m and c.

It is well known that one of the important aspects of the validity of exact results is the following: they may be used as trial results for evaluation of accuracy of approximate methods. Therefore, the exact results for plates with equations (7.1) may be used for evaluation of approximate methods which are oriented to the numerical solution of spectral problems for non-homogeneous bodies (FEM, FDM and others). Examples are given in Appendix 6.

(iii) It is possible to show that optimization inequalities can be generalized to various problems connected with transversal impact [26] and forced vibration [27].

(iv) The relations described can be generalized to a linear viscoelastic plate with a non-elastic foundation, on a foundation with "one-sign-reaction" (see, e.g., reference [28]), and to plane problems of elasticity and linear viscoelasticity.

(v) In Appendix 3, the triangular plate with a clamped contour is considered, and it is noted that the position of a point mass, which minimizes the eigenfrequency, satisfies the inequality (3.2). In section 6 the annular plate with both contours clamped and with uniformly distributed mass was considered and it was shown numerically (Figure 4) that the "best" radii of ring-supports (elastic and rigid) are greater than the radius of inversion symmetry of plate domain $r_s = (r_{out} r_{int})^{1/2}$. In Appendix 5 it is noted that the same situation exists if the plate outer contour clamping is replaced by simple supporting.

In all the above-listed examples, the plates are non-inversion-symmetric, but the inequalities of sections 3 and 5 are valid. It is possible to give many such examples. From the physics and engineering point of view, it is easy to show such evident "disturbances" (of contour, boundary conditions, mass distribution, stiffness distribution, etc.) of inversion-symmetric plates, which "destroy" the plate symmetry, but which produce the optimal point "motion" in the only "away-direction" from the symmetry-circle of the initial plate. For such plates, the inequalities of sections 3 and 5 retain their validity. Therefore, these inequalities may be considered as a starting point for the optimization of many real non-symmetric plates.

ACKNOWLEDGMENT

The authors are grateful to Evgenia Ioffe and Yetta Klyachko for their help.

REFERENCES

1. J. H. Mitchell 1902 *Proceedings of the London Mathematical Society* **34**, 134–142. The inversion of plane stress.
2. J. H. Mitchell 1902 *Proceedings of the London Mathematical Society* **34**, 223–238. The flexure of a circular plate.
3. R. D. Mindlin 1937 *Journal of Applied Mechanics* **4**, A-115–A-118. Stress systems in a circular disk under radial forces.
4. W. Olszak and Z. Mroz 1957 *Archiwum Mechaniki Stosowanej* **9**, 125–153. Elastic bending of circular plates with eccentric holes (application of the method of inversion).
5. W. Olszak 1958 *Archiwum Mechaniki Stosowanej* **10**, 417–440. The inversion mapping as applied in the theory of plasticity.

6. V. T. Buchvald 1963 *Mathematika* (*Journal of Pure and Applied Mathematics*, *London*) **10**, 29–34. Plane elastostatic boundary-value problems, part 2: the role of inversion.
7. S. D. Klyachko 1974 *Journal of Applied Mechanics and Technical Physics* **13**, 250–252. Use of inversion transformation for modeling in certain problems of the theory of elasticity and plasticity. (New York: Consultants Bureau; translated from Russian).
8. H. P. W. Gottlieb 1991 *Transactions of the American Society of Mechanical Engineers*, *Journal of Applied Mechanics* **58**, 729–730. Inhomogeneous clamped circular plates with standard vibration spectra.
9. H. P. W. Gottlieb 1992 *IMA Journal of Applied Mathematics* **49**, 185–192. Axisymmetric isospectral annular plates and membranes.
10. V. S. Sarkisian 1976 *Some Problems of the Mathematical Theory of Elasticity of Anisotropic Body*. Erevan: Erevan University (in Russian).
11. S. Abrate and E. Foster 1995 *Journal of Sound and Vibration* **179**, 793–815. Vibrations of composite plates with intermediate line support.
12. K. M. Liew and K. Y. Lam 1994 *Journal of Sound and Vibration* **174**, 23–26. Effects of arbitrary distributed elastic point constraints on vibrational behaviour of rectangular plates.
13. R. Y. Bodine 1967 *Journal of the Acoustical Society of America* **41**, 1551. Vibrations of a circular plate supported by a concentric ring of arbitrary radius.
14. V. X. Kunukkasseril and A. S. J. Swamidas 1974 *International Journal of Solids and Structures* **10**, 603–619. Vibration of continuous circular plates.
15. Y. Narita 1984 *Journal of Sound and Vibration* **93**, 503–511. Variations of frequency parameters for plate with supporting location.
16. S. Azimi 1988 *Journal of Sound and Vibration* **120**, 37–52. Free vibration of circular plates with elastic or rigid interior supports.
17. C. S. Kim and S. M. Dickinson 1989 *Journal of Sound and Vibration* **130**, 363–377. On the lateral vibration of thin annular and circular composite plates subject to certain complicated effects.
18. T. S. Shih and D. Allaei 1990 *Journal of Sound and Vibration* **140**, 239–257. On the free vibration of annular plates with ring-type elastic attachments.
19. E. E. Allen 1954 *Mathematical Tables and other Aids to Computation* **8**, 240–241. Analytical approximations.
20. E. E. Allen 1956 *Mathematical Tables and other Aids to Computation* **10**, 162–164. Polynomial approximations to some modified Bessel functions.
21. M. Abramowitz and I. A. Stegun 1964 *Handbook of Mathematical Functions*. Gaithersburg, MD: U.S. National Bureau of Standards.
22. S. M. Vogel and D. W. Skinner 1965 *Transactions of the American Society of Mechanical Engineers* (*E*), *Journal of Applied Mechanics* **32**, 926–931. Natural frequencies of transversely vibrating uniform annular plates.
23. A. W. Leissa 1969 *Vibration of Plates*. Washington, D.C.: NASA (*Science paper SP-160*).
24. R. Lal and U. S. Gupta 1982 *Journal of Sound and Vibration* **83**, 229–240. Axisymmetric vibrations of polar orthotropic annular plates of variable thickness.
25. J. B. Greenberg and Y. Stavsky 1979 *Journal of the Acoustical Society of America* **66**, 501–508. Flexural vibrations of certain full and annular composite orthotropic plates.
26. E. Wu and C.-S. Yen 1992 18*th International Congress of Theoretical and Applied Mechanics Haifa*, *Israel*, 159 Detection of impact force history and location on a laminated plate.
27. G. Kemper 1974 *Acustica* **30**, 173–179. The position dependence of the input power for point-shaped excited plate vibration.
28. Z. Celep and D. Turhan 1990 *Transactions of the American Society of Mechanical Engineers*, *Journal of Applied Mechanics* **57**, 677–681 Axisymmetric vibrations of circular plates on tensionless elastic foundations.
29. C. Fang and G. C. Springer 1993 *Journal of Composite Materials* **27**, 721–753. Design of composite laminates by a Monte Carlo method.

APPENDIX 1

(i) Here we prove the invariance of equation (2.1) under the transformation (2.2) stated in section 2. As is known, the invariance of an equation

$$F(x, u, a) = 0, \tag{A1.1}$$

where x, u and a are argument, function and parameter; under some transformation

$$x^* = f_x(x), \qquad u^* = f_u(u), \qquad a^* = f_a(a), \tag{A1.2}$$

means the following. We say that (A1.1) is invariant under (A1.2) if

$$F[f_x^{-1}(x^*), f_u^{-1}(u^*), f_a^{-1}(a^*)] = 0 \leftrightarrow F(x^*, u^*, a^*) = 0. \tag{A1.3}$$

We return to expressions (2.1) and (1.2). We express from equations (2.2) the quantities without an "asterisk" in terms of those with "an asterisk". After substituting these expressions in equation (2.1), taking into account condition (2.3) and making some identical transformations one obtains the same equation (2.1), but in which all quantities, except the D^{ijkl}, are replaced by those with "an asterisk". This finishes the proof. For the homogeneous isotropic case it was proved in references [2, 4], and for the homogeneous orthotropic case in reference [7].

(ii) In section 2 it is noted that for industrial materials reinforced only in the radial direction the quantity $D^{1122}(\theta) + D^{2222}(\theta)$ changes weakly in comparison with $D^{1111}(\theta)$. Therefore, for those materials the condition (2.3) may be approximately accepted and the invariance of equation (2.1) under transformation (2.2) may be used. Here we give two examples of such a material. Note again that the reinforcement here is such that stiffness tensor co-ordinates $D^{ijkl}(\theta)$ related to the local orthonormal basis are independent of r and are functions of only θ.

(ii, 1) *Example* 1. Consider a "classical" idealized three-layer plate, in which the plate bending rigidity $D^{ijkl}(\theta)$ is generated only by in-plane rigidities of two outer thin layers. The distance between outer layers $h = \text{constant} \gg \delta(\theta)$, where $\delta(\theta)$ is the thickness of one layer (both layers are the same). Each outer layer is fabricated from isotropic and orthotropic sublayers with thicknesses $\delta_{is} = \text{constant}$ and $\delta_{or} = \delta_{or}(\theta)$. Therefore, $\delta(\theta) = \delta_{is} + \delta_{or}(\theta)$. The material stiffness tensors are constant: $T_{is}^{ijkl}{}_{,\theta} = T_{or}^{ijkl}{}_{,\theta} = 0$. Note that $T_{is}^{1111} = T_{is}^{2222} = T_{is}$; $T_{is}^{1122} = \mu T_{is}$; $T_{is}^{1212} = 0{\cdot}5(1-\mu)T_{is} = G$; $T_{is} = E/(1-\mu^2)$ and $T_{or}^{1111} = E_1/(1-\mu_1\mu_2)$; $T_{or}^{2222} = E_2/(1-\mu_1\mu_2)$; $T_{or}^{1122} = \mu_1 E_1/(1-\mu_1\mu_2)$; $T_{or}^{1212} = G_{12}$; $\mu_1 E_1 = \mu_2 E_2$. Therefore

$$D^{ijkl}(\theta) = [T_{is}^{ijkl}\delta_{is} + T_{or}^{ijkl}\delta_{or}(\theta)]h^2/2. \tag{A1.4}$$

For evaluation of a change of $D^{1122}(\theta) + D^{2222}(\theta)$ one must compare it with a change of $D^{1111}(\theta)$. Let θ_{min} and θ_{max} be some values of θ and let the orthotropic sublayer thickness be such that

$$\delta_{or}(\theta_{min}) = \delta_{or\,min} = 0, \qquad \delta_{or}(\theta_{max}) = \delta_{or\,max}, \tag{A1.5}$$

where $\delta_{or\,max}$ is some value. With these assumption and this notation we can write, from equation (A1.4)

$$D^{ijkl}(\theta_{min}) = T_{is}^{ijkl}\delta_{is}h^2/2, \tag{A1.6}$$

$$D^{ijkl}(\theta_{max}) = [T_{is}^{ijkl}\delta_{is} + T_{or}^{ijkl}\delta_{or\,max}]h^2/2. \tag{A1.7}$$

Now write

$$k = D^{1111}(\theta_{max})/D^{1111}(\theta_{min}), \tag{A1.8}$$

$$p = [D^{1122}(\theta_{max}) + D^{2222}(\theta_{max})]/[D^{1122}(\theta_{min}) + D^{2222}(\theta_{min})]. \tag{A1.9}$$

The parameters k and p represent the increasing of $D^{1111}(\theta)$ and $D^{1122}(\theta) + D^{2222}(\theta)$, respectively, by "going" from θ_{min} to θ_{max}. It is clear that if one writes the relation $p = p(k)$, one will be able to compare p and k: i.e., the "evaluation problem" will be solved.

Rewrite equations (A1.8) and (A1.9) with the help of equations (A1.6) and (A1.7) as

$$k = 1 + (T_{or}^{1111}/T_{is}^{1111})\delta_{or\,max}/\delta_{is}, \tag{A1.10}$$

$$p = 1 + [(T_{or}^{1122} + T_{or}^{2222})/(T_{is}^{1122} + T_{is}^{2222})]\delta_{or\,max}/\delta_{is}. \tag{A1.11}$$

Expressing $\delta_{or\,max}$ from equation (A1.10) and substituting it in equation (A1.11), one obtains

$$p = 1 + (k-1)[(T_{or}^{1122} + T_{or}^{2222})/T_{or}^{1111}]^{+1}[(T_{is}^{1122} + T_{is}^{2222})/T_{is}^{1111}]^{-1}, \tag{A1.12}$$

or, in "technical" form,

$$p = 1 + (k-1)[(\mu_2 + 1)E_2/E_1]/(\mu + 1). \tag{A1.13}$$

Relation (A1.13) is the answer to the question.

Now consider some numbers. Take an isotropic material with a "typical" Poisson ratio of $\mu = 0{\cdot}3$. As an orthotropic material, take, e.g., from reference [29], graphite–epoxy plies with $E_1 = 181{\cdot}0$ GPa, $E_2 = 10{\cdot}30$ GPa, $\mu_2 = 0{\cdot}28$ and $G_{12} = 7{\cdot}17$ GPa. Let $k = 1{\cdot}5$, for example. Then, from equation (A1.13), $p = 1{\cdot}028$. This means that if $D^{1111}(\theta)$ increases (by "going" from θ_{min} to θ_{max}) by 1·5 times, then the value of $D^{1122}(\theta) + D^{2222}(\theta)$ increases by only 2·8%. Therefore, one can accept

$$D^{1122}(\theta) + D^{2222}(\theta) \approx \text{constant}. \tag{A1.14}$$

(ii, 2) *Example* 2. Consider as a second example of material (A1.14), another "classical" type of sandwich plates. In reference [25] an annular three-layer plate is considered, in which the middle layer is steel ($\mu = 0{\cdot}33$) or aluminium ($\mu = 0{\cdot}22$) and the outer layers are "Ultra-high-modulus graphite–epoxy"—UMGE ($E_1 = 310$ GPa, $E_2 = 6{\cdot}2$ GPa, $\mu_2 = 0{\cdot}26$, $G_{12} = 4{\cdot}1$ GPa). Let $h =$ constant and $\delta(\theta)$ be the thicknesses of the inner and outer layers. For such a plate,

$$D^{ijkl}(\theta) = T_{is}^{ijkl}\int_{-h/2}^{+h/2} z^2\,\mathrm{d}z + 2T_{or}^{ijkl}\int_{+h/2}^{+h/2+\delta(\theta)} z^2\,\mathrm{d}z. \tag{A1.15}$$

Let θ_{min} and θ_{max} again be two values of θ and let $\delta(\theta_{min}) = 0$. It is easy to show that for plate (A1.15) the relations (A1.12) and (A1.13) are valid. Assuming $k = 1{\cdot}5$ again and substituting the materials' numerical data in equation (A1.13), one finds that $p = 1{\cdot}0098$ (for steel) and $p = 1{\cdot}0103$ (for aluminium). This means again that if $D^{1111}(\theta)$ increases by 1·5 times, the sum $D^{1122}(\theta) + D^{2222}(\theta)$ increases by only $\approx 1\%$.

These two examples show that for very well known classes of materials reinforced only in the r direction $D^{ijkl}(\theta)$ one can accept equation (A1.14) approximately, and use all benefits, which are generated by the inversion-invariance stated in section 2. For other materials and kinds of reinforcement, the sum $D^{1122}(\theta) + D^{2222}(\theta)$ may be even nearer to a constant. Recall again that if the plate is homogeneous, then the polar-orthotropic tensor D^{ijkl} may be otherwise arbitrary.

APPENDIX 2

(i) Here the inequality (3.2) (see section 3) is proved. The considered plate has one dynamical degree of freedom, so

$$\omega = (MG(\alpha_M, \alpha_M))^{-1/2}, \tag{A2.1}$$

where $G(\alpha, \beta)$ is the Green function of the static problem. From plate symmetry and expression (2.2) it follows that

$$G(\alpha^*, \alpha^*) = (r_s/r_\alpha)^4 G(\alpha, \alpha): \tag{A2.2}$$

i.e., if $r_\alpha < r_s$, then

$$G(\alpha^*, \alpha^*) > G(\alpha, \alpha). \tag{A2.3}$$

After differentiation of both sides of equation (A2.2) with respect to r, one finds that if $r = r_s$, then $\mathrm{d}G(r, \theta; r, \theta)/\mathrm{d}r \neq 0$. This finishes the proof.

(ii) Often in applications the optimization aim is to maximize ω, but not to minimize it. Without reference to the relative complexity of these two problems, consider an extended formulation. Let domain $B \subset A$ (such that $\partial B \cap \partial A = \varnothing$) be an arbitrary given interior domain. Denote $C_{out} = (B + \partial B) \cap (r > r_s)$; $C_{int} = (B + \partial B) \cap (r < r_s)$ and $C_{mid} = \partial B \cap (r = r_s)$.

Consider the following optimization problem: find $\alpha_{Mmin} \in B + \partial B$ and $\alpha_{Mmax} \in B + \partial B$ such that, for all $\alpha_M \in B + \partial B$, $\omega(\alpha_{Mmin}) \leqslant \omega(\alpha_M) \leqslant \omega(\alpha_{Mmax})$.

It is possible to show that

$$\alpha_{Mmin} \in C_{out} + C_{int} \big\backslash C^*_{out} + C_{mid}, \qquad \alpha_{Mmax} \in C_{int} + C_{out} \big\backslash C^*_{int} + C_{mid}, \tag{A2.4}$$

where "the asterisk" means the inversion image (see above). The proof is analogous to that of inequality (3.2). If B is symmetric, i.e., $B^* = B$, then $C_{int} = C^*_{\mathrm{out}}$ and expressions (A2.4) reduce to

$$\alpha_{Mmin} \in (B + \partial B) \cap (r > r_s) + \partial B \cap (r = r_s),$$
$$\alpha_{Mmax} \in (B + \partial B) \cap (r < r_s) + \partial B \cap (r = r_s). \tag{A2.5}$$

If ∂B is such that at all points $b \in \partial B \cap (r = r_s)$ the radius is tangential to ∂B, then the last terms in expressions (A2.4) and (A2.5) may be cancelled. Note the results of section 3 and Appendix 2 are generalized (in some sense) in the case of a polyharmonic equation.

"Near" statements may be given for various formulations of optimizations problems in cases of a mass system and continuously distributed mass and elastic foundation.

APPENDIX 3

In section 4, the inequality (3.2) was illustrated by two examples of inversion-symmetric plates. Here an example is given of the validity of inequality (3.2) for the case of a non-inversion-symmetric plate. Consider a segment plate 1–3–5 with $\beta < 90^\circ$ (see Figure 2). Draw tangents to arc 1–3–5 at points 1 and 5, and denote the intersection points as 11 (in Figure 2 these tangents and point 11 are not shown). Thus, one obtains the isosceles triangle 1–11–5. Let this be a triangular plate with a clamped contour. From the physics point of view it is clear that by "transformation" of the segment plate 1–3–5 into triangle 1–11–5 the "best" point will "move" in a direction away from the symmetry circle. Therefore inequality (3.2) will retain its validity. It is easy to give other similar examples.

APPENDIX 4

Here, a proof of the inequality (5.1) of section 5 is presented. Let the support, which has the given stiffness coefficient C and is located at point α_{Cmax} with $r_{Cmax} < r_s$, generates the eigenfrequency $\omega^{(1)}(\alpha_{Cmax})$ such that, for all points α_C, $\omega^{(1)}(\alpha_C) \leqslant \omega^{(1)}(\alpha_{Cmax})$. According to expression (2.2), there exists the same plate, but with support at the symmetrical point α^*_{Cmax} with $r_{Cmax} > r_s$, which has the same $\omega^{(1)}(\alpha^*_{Cmax}) = \omega^{(1)}(\alpha_{Cmax})$. The stiffness coefficient of the new support $C^* < C$ (according to expression (2.2)). Now increase the stiffness coefficient of the new support up to the given level C. As is known, addition to the stiffness

coefficient of some part of an elastic system does not decrease the eigenfrequency. This finishes the proof. Proofs of other statements of section 5 are similar to the given proof.

APPENDIX 5

(i) DESCRIPTION OF NUMERICAL METHOD USED IN SECTION 6

A version of the initial parameters method is used. The solution on $A + B$ is represented as $w_{nd}(\xi, \lambda) = P^{[1]}w^{[1]}(\xi, \lambda) + P^{[2]}w^{[2]}(\xi, \lambda)$, where $w^{[i]}$ are solutions of the Cauchy problem for equation (6.6) with "standard" initial conditions $\{0; 0; 1; 0\}$, $\{0; 0; 0; 1\}$ at point $\xi = \xi_{int}$ and with "jumps" $\Delta w^{[i]}_{,\xi\xi\xi}$ (6.10) at point $\xi = \xi_{sup}$ (case $C_{nd} = \infty$ has some evident distinctions); $P^{[i]}$ satisfy the system, which is generated by the boundary conditions (6.8) at point $\xi = 1$; the eigenfrequency λ is obtained from the characteristic equation $F(\lambda) = 0 (\lambda_- \leqslant \lambda \leqslant \lambda_+)$, where $F(\lambda)$ is the determinant of a 2-matrix and λ_- and λ_+ are known limits. The Cauchy problem for equation (6.6) is solved by an often exploited version of the Runge–Kutta method: equation (6.6) is reduced to a system $y^{(i)} = f^{(i)}(\xi, y^{(1)}, \ldots, y^{(4)})$ and the known algorithm $y^{(i)}_{n+1} = y^{(i)}_n + (\Delta\xi/6)(k^{(i)}_1 + 2k^{(i)}_2 + 2k^{(i)}_3 + k^{(i)}_4)$ is used. The numbers of ξ-steps in the subdomains n^A_{step} and n^B_{step} are determined on the basis of an assumed general number of steps $n_{step} = n^A_{step} + n^B_{step}$ in proportion to the lengths of the subdomains (with rounding). In all calculations below it is assumed that $n_{step} = 100$ and the 8-byte size of numbers (Borland Turbo-Pascal) is used.

(ii) TESTING OF THE NUMERICAL METHOD

The approximate initial parameters method based on the Cauchy problem solution by the Runge–Kutta procedure described above is applied to a plate with $\xi_{int} = 0{\cdot}5$, $\xi_{sup} = 0{\cdot}75$, $D^{2222}_{nd} = 1$ and $m_{nd} = 1$, and the function $\lambda(C_{nd})$ is constructed. The same function is constructed by an "exact" method based on the Bessel functions polynomial approximation [19–21]. As was assumed in section 6, the numerical method and "exact" one used are denoted as the methods N and E (and, if necessary, the letters N and E will be used as indices). After comparison, it turns out that

$$|\lambda_N - \lambda_E| < 0{\cdot}001. \tag{A5.1}$$

Values of λ with two digits after the decimal point (i.e., digits generated by method N as well as by method E) are given in Table 1.

Additional testing is based on results from some publications. The case $\xi_{int} = 0{\cdot}5$, $D^{2222}_{nd} = 1$, $C_{nd} = 0$ and $m_{nd} = 1$ was considered in reference [22] (see also reference [23]) by using the Bessel functions approximation (the result is $\lambda = 89{\cdot}2$), in reference [24] by using the Chebyshev polynomial approximation solution (the result was given in graphical form), in reference [17] by using the Rayleigh–Ritz method with the Chebyshev polynomial approximation (the result is $\lambda = 89{\cdot}251$) and in reference [18] by using the Galerkin method with a finite element model (the result is $\lambda = 89{\cdot}25$). Our result is $\lambda = 89{\cdot}25$ (obtained by both methods N and E; condition (A5.1) is satisfied). The difference between this value and the graphical result of reference [24] is no greater than 1%.

The case $\xi_{int} = 0{\cdot}5$, $D^{2222}_{nd} = 10$, $C_{nd} = 0$ and $m_{nd} = 1$ was considered in reference [24] by using the Chebyshev polynomial approximation solution (the result was given graphically). Our result is $\lambda = 93{\cdot}82$ (obtained by the N-method). The difference is no greater than 1%.

The case $\xi_{int} = 0{\cdot}3$, $\xi_{sup} = 0{\cdot}5$, $C_{nd} = \infty$, $m_{nd} = 1$ and $D^{2222}_{nd} = \{0{\cdot}02; 50\}$ was considered in reference [17] by using the Rayleigh–Ritz method with the Chebyshev polynomial approximation. Values of D^{2222}_{nd} correspond to the two orientations of "Ultra-high-modulus graphite–epoxy", UMGE, and are taken from reference [25]. The result is

$\lambda = \{77{\cdot}562; 104{\cdot}01\}$. Our result is $\lambda = \{77{\cdot}42; 103{\cdot}76\}$ (obtained by the N-method). Additionally, we considered the isotropic case $D_{nd}^{2222} = 1$ and obtained the result $\lambda = 78{\cdot}05$ (by methods N and E; condition (A5.1) is satisfied).

Comparisons with E-method results and with results of the publications mentioned show that the N-method with $n_{step} = 100$ has a sufficient accuracy.

(iii) ABOUT EXTENSION OF THE RESULTS OF SECTION 5 ON NON-INVERSION-SYMMETRIC PLATES

Inequality (5.1) is valid not only for inversion-symmetric plates. As an example, consider the plate with ISMD (6.3) considered in section 5. Decrease the mass density in the subdomain $r \leqslant r_s$ from $m_0(r_s/r)^{+8}$ to a value m_0; in other words, transform (by the removal of "excess" mass) the plate with ISMD into the plate with $m = m_0 =$ constant (the uniform mass distribution is not inversion-symmetric). It is clear that by such a change of the plate the inequality (5.1), $\xi_{sup\,max} \geqslant \xi_s$ remains in force (for an illustration, see Table 4 and Figure 4). It is also clear that there exists an infinite class of analogous changes of mass distribution, for which the inequality (5.1) is valid. To give another example, replace the rigid clamping on the outer contour by simple supporting. It is clear that such a transformation of boundary conditions retains the validity of the results of section 5. Therefore, one can say that there exist such evident changes in mass distribution, boundary conditions, plate contour, elasticity tensor D^{ijkl}, and so on, which transform the inversion-symmetric plate into a non-inversion-symmetric one, for which the results of section 5 remain valid.

APPENDIX 6

In section 7 it was noted that an arbitrary plate with mass distribution (7.1) is isospectral to a plate with uniformly distributed mass. It was also noted that this statement may be used for testing of numerical methods. Here this possibility is illustrated.

Return to section 6 and consider the plate with $m_{nd} \equiv 1$, $\xi_{int} = 0{\cdot}5$, $D_{nd}^{2222} = 1$, $C_{nd} = \infty$ and $\xi_{sup} = 0{\cdot}75$. The result, i.e., λ, was obtained (see Table 1) by exact and numerical methods (the E-method- and the N-method): $\lambda_{\mathrm{E}} = 246{\cdot}34271$ and $\lambda_{\mathrm{N}} = 246{\cdot}34287$ (here more digits are given than in Table 1). Therefore, one can say that the N-method, applied to the plate with $m_{nd} \equiv 1$, gives satisfactory results. However, what is the accuracy of the N-method if $m_{nd} = m_{nd}(\xi)$? The answer may be obtained if one has some plate with $m_{nd}(\xi)$ for which the exact solution is known.

Relation (7.1) provides such a possibility. After inversion-transformation with respect to the circle of ξ_s one obtains the plate with $m_{nd}^* = (\xi_s/\xi)^{+8}$, $\xi_{int} = 0{\cdot}5$, $D_{nd}^{2222} = 1$, $C_{nd}^* = \infty$ and $\xi_{sup}^* = (\xi_s)^2/\xi_{sup} = 2/3$. (Note that this $m_{nd}^*(\xi)$ is a "very" non-uniform distribution: $m_{nd}^*(\xi_{int}) = 16$, $m_{nd}^*(\xi_{out}) = 0{\cdot}0625$.)

For this plate, according to expression (7.1), $\lambda_{\mathrm{E}}^* = \lambda_{\mathrm{E}}$. Therefore, one has a plate with non-uniform m_{nd}^* and with known λ_{E}^*. After application of the N-method to this plate, one obtains $\lambda_A^* = 246{\cdot}34324$. Evidently, the absolute error is 3·3 times greater than that for the case $m_{nd} = 1$, but (because of the negligibly small relative error) the N-method with $n_{step} = 100$ may be considered as a satisfactory approach. Therefore, this statement of section 7 helps to indicate the possible applicability of numerical methods to problems with a non-uniform mass distribution.